Mode-field adapter for tapered-fiber-bundle signal and pump combiners

Pavel Koška,[1,2,*] Yauhen Baravets,[1,2] Pavel Peterka,[1] Jan Bohata,[3] and Michael Písařík[3]

[1]Institute of Photonics and Electronics ASCR, v.v.i., Chaberská 57, Prague 18251, Czech Republic

[2]Department of Physical Electronics, Czech Technical University in Prague, Břehová 7, Prague 11519, Czech Republic

[3]Department of Electromagnetic Field, Czech Technical University in Prague, Technická 2, Prague 16627, Czech Republic

*Corresponding author: koska@ufe.cz

Received 28 August 2014; revised 16 December 2014; accepted 16 December 2014; posted 16 December 2014 (Doc. ID 221872); published 26 January 2015

We report on a novel mode-field adapter that is proposed to be incorporated inside tapered fused-fiber-bundle pump and signal combiners for high-power double-clad fiber lasers. Such an adapter allows optimization of signal-mode-field matching on the input and output fibers. Correspondingly, losses of the combiner signal branch are significantly reduced. The mode-field adapter optimization procedure is demonstrated on a combiner based on commercially available fibers. Signal wavelengths of 1.55 and 2 μm are considered. The losses can be further improved by using specially designed intermediate fiber and by dopant diffusion during splicing as confirmed by preliminary experimental results. © 2015 Optical Society of America

OCIS codes: (060.2340) Fiber optics components; (060.3510) Lasers, fiber; (060.2320) Fiber optics amplifiers and oscillators.

http://dx.doi.org/10.1364/AO.54.000751

1. Introduction

High-power fiber lasers are gaining importance in many fields, including industrial material processing, metrology, and health care. The key for high-power operation of fiber lasers is the usage of double-clad fibers (DCFs) as transformers of lower-brightness pumps into high-brightness laser signal beams [1,2]. Pumping radiation needs to be introduced into the first cladding of the DCF while the active core of the DCF often needs to be accessible by dedicated signal fiber. Pump-signal combiners are devices responsible for such coupling and they are thus crucial components of high-power fiber lasers. Several approaches were developed for pump and signal coupling into DCFs [3–18]. Combiners utilizing free-space optics are usually impractical out of the laboratory environment due to lack of robustness [3]. The free-space-optics combiner was used by Elias Snitzer in the first demonstration of a cladding-pumped fiber laser [2] but very soon an all-fiber solution was envisaged by Gapontsev [4] and later demonstrated by using a tapered pump fiber wrapped around the DC fiber [5]. The pump can be coupled from the side of the DC fiber by using a tapered capillary [6], or prism [7]. Pump coupling from the end of the DC fiber can be achieved, e.g., by using a specially designed input fiber (IF) with smaller diameter than the output DC fiber; the IF is surrounded by pretapered multimode fibers for the pump [8]. Low-loss end-pumping was demonstrated by using direct splicing of pump and signal fibers into the DC fiber with stadium-like cross section [9]. Other methods consist of bundling individual and separable pump and signal fibers where the pump radiation couples between the fibers; the fibers are tightly touching thanks to a heat-shrunk tube over the fibers [10] or by twisting

1559-128X/15/040751-06$15.00/0

the fiber bundle [11,12]. Among the most suitable solutions for practical applications are fused fiber bundle combiners [13]. These combiners consist of several multimode pump delivery fibers and a signal fiber. Fibers are bundled together and then fused and tapered to match the output DCF [14]. Instead of multimode-laser-diode pumps, the plurality single-mode fiber lasers can be also combined in the so-called tandem pumping scheme that enables operation of a high-power fiber amplifier to deliver a power of up to 20 kW [15].

Methods for achieving low losses in the signal branch of the combiner are of increasing importance in order to improve efficiency and reliability of fiber laser systems. Reduction of losses requires accurate field profile matching both on input and output of the combiner. Because of tapering, the mode-field profile changes in the signal fiber along the taper and the problem with field profile matching arises. Several approaches addressing this problem were proposed. At first, a special fiber with matched mode-field profile simultaneously on input and output was discussed as a signal fiber in [13]. The signal fiber is connected to the IF before the fused portion of the combiner and to the output fiber (OF) at the end of the fused portion of the combiner in this case. Limitations of the mode-field matching of such a signal fiber connection are obvious from later analysis provided by Kong *et al.* [19]. The second technique consists of fattening of the signal fiber core before bundling and tapering, which is achieved by heating and subsequent dopant diffusion [14]. The third approach is based on vanishing core technology when the special DCF is used as the signal fiber inside the combiner [16,17]. By tapering, the field expands from the core to the first cladding, which is matched to the OF core at the end of the taper. Another approach consists of etched taper conserving core diameter along the taper [18].

In this paper we propose and demonstrate a mode-field adapter that is based on tapered splice between dissimilar fibers inside the bundled pump and signal combiner. A similar technique was also proposed for the reduction of splicing loss between a single-mode fiber and a dispersion-flattened fiber where splice losses were reduced by moderate tapering of the splice itself [20] and for low-loss splice in a wavelength-independent Y-junction beam splitter [21]. Here, we utilized to the best of our knowledge for the first time the splice tapering principle inside the bundled pump and signal combiner. Placement of the splice inside the tapered part of the combiner introduces an additional degree of freedom in comparison with [13]. Optimization of the splice position inside the taper extends the range of possibilities of combiner losses reduction and it provides a way to improve the reliability of the combiners in high-power fiber lasers.

2. Combiner Principle and Design

The proposed tapered fiber bundle combiner is schematically shown in Fig. 1. The bundle combiner consists of several pump delivery fibers and one signal fiber. A single-mode fiber is used as the signal input. Inside the tapered part of the bundle the signal IF is spliced to the appropriate intermediate fiber (MF). The tapered bundle is spliced to active or passive double-clad OF.

The principle of operation is as follows. As the IF is tapered, the field first shrinks and then expands from the core. The mode-field diameter (MFD) becomes even greater than that of the original nontapered fiber below a certain taper ratio. The splice is placed at the point where the IF expanded field profile corresponds to the field profile of the MF tapered with the same ratio. The MF is further tapered with the bundle to the point where the diameter of the bundle corresponds to the diameter of the OF. The MFD in the MF decreases in the progressing down-taper portion. The field profile at the end of the MF must correspond to the field profile of the OF core. Therefore, the choice of the MF is crucial for successful design.

A. Numerical Design

In order to clarify the design procedure let us describe the particular design of geometrically hexagonal $(6+1)\times 1$ combiner signal branch for the wavelengths of 2 and 1.55 μm. We assume standard single-mode fiber according to ITU recommendation G.652 as the IF, e.g., the Corning SMF28 fiber with the numerical aperture (NA) of 0.14, the core diameter of 8.2 μm, and the cladding diameter of 125 μm. On the output, we assume the OF with core mode-field profile matched to SMF28 and cladding diameter of 125 μm. Because the bundle consists of seven fibers, it needs to be tapered to the ratio of 1/3 to match the diameter of the OF. The MF is required to have its field profile matched to the OF at the end of the taper. The easiest way is to use a special fiber with core and cladding refractive indices corresponding to the OF, but a threefold larger core diameter. In a theoretical case, when we neglect perturbations of fiber NA and core diameter due to dopant diffusion during fabrication and splicing processes, such a special fiber fundamental mode will have exactly the

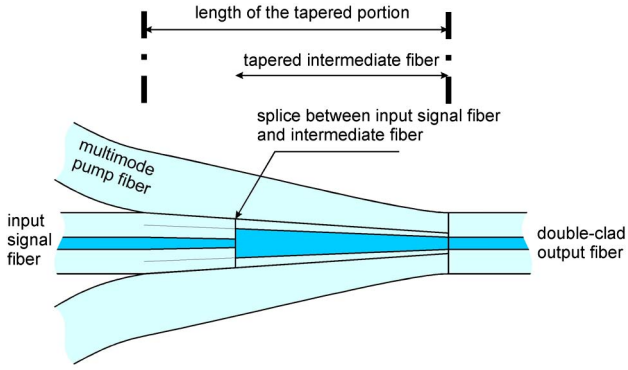

Fig. 1. Schematic illustration of the proposed mode field adapter inside the bundled tapered pump and signal combiner.

same field profile as the OF when tapered to the ratio of 1/3.

Commercially available fiber can be also used instead of a special fiber. The fiber should have approximately a threefold larger core and similar NA with respect to the OF. The suitability of the fiber needs to be verified using numerical simulation. In our particular case, we used CorActive MM-20/125 fiber [22] with NA 0.14 for the wavelength of 2 μm and CorActive SCF-UN 20/125-12 fiber [22] with NA 0.12 for the wavelength of 1.55 μm. We started with the fundamental LP_{01} eigenmode of each fiber and used the finite element beam propagation method [23,24] to calculate the field distribution evolution along the fibers tapered to the ratio of 1/3. The taper had linear shape and the length of the taper was 12 mm, so the taper was gradual and adiabatic [25]. We then calculated the fundamental eigenmode of the standard single-mode fiber, which according to our assumption corresponds to the eigenmode of the OF. Finally, we calculated the overlap integral (1) between OF eigenmode and the propagated field in each propagation step. The result quantifies the field correspondence between the OF and the MF with respect to the tapering ratio. Splice loss is determined by the squared absolute value of the overlap integral [26,27] and it is shown in Fig. 2.

$$a = \frac{\int \vec{E}_1 \vec{E}_2^* \mathrm{d}\Omega}{\sqrt{\int |\vec{E}_1|^2 \mathrm{d}\Omega}\sqrt{\int |\vec{E}_2|^2 \mathrm{d}\Omega}}. \quad (1)$$

Figure 2 shows that minimal splice loss is achieved slightly before the target ratio for both wavelengths, but loss at the ratio of 1/3 is not significantly worse.

The second step is finding the optimal position of the splice between the tapered IF and the MF. The splice must be placed to the point of optimal field matching between both fibers. Again, we started with fundamental LP_{01} eigenmode of each fiber and used the beam propagation method for calculating the field profile evolutions in the tapered input and MFs. Then we calculated the overlap integral

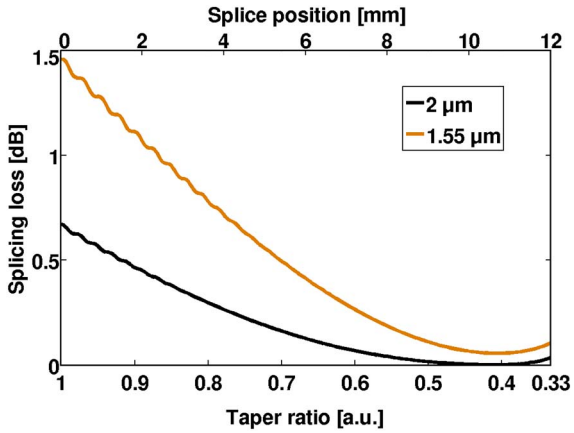

Fig. 2. Estimation of MF—OF splicing loss dependence on MF tapering ratio and splice position.

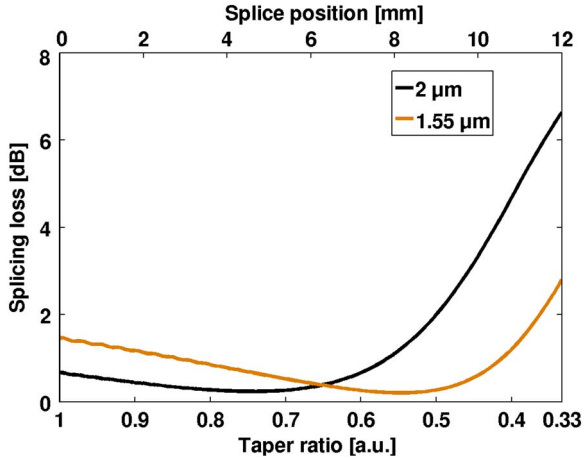

Fig. 3. Estimation of splice loss dependence on taper ratio and splice position between IF and MF based on squared absolute value of overlap integral between fields in fibers.

between fields of these tapered fibers for each taper ratio. Figure 3 shows the dependence of the estimated splice loss on the taper ratio between the IF and the MF.

Minimum loss is achieved for the ratio of 0.74 for 2 μm design and for the ratio of 0.55 in the case of 1.55 μm design. Loss is approximately 0.2 dB in both cases. The actual position of the splice (place of the optimum taper ratio) along the taper depends on the shape of the taper. In our simulations we assumed adiabatic linear taper with the length of 12 mm. So the optimal positions for splices were 4.7 mm from beginning for 2 μm design and 8.2 mm from beginning for 1.55 μm design. In general, the shape of the taper is not important as long as the taper is adiabatic [25].

Finally, we verified the proposed design. We excited the designed adapters by IFs fundamental LP_{01} eigenmodes for both wavelengths and evaluated overlap integrals between fundamental LP_{01} modes of the OFs and fields propagated along the adapters. Evolution of overlap integrals along the adapters is shown in Fig. 4. Transmittances of adapters correspond to the squared absolute value of the overlap integrals values at the end of propagation. Figure 4 shows that the transmittances of −0.27 dB in the case of 2 μm and −0.37 dB for 1.55 μm are achieved between IFs and OFs. The evolution of optical intensity along the taper is illustrated in Fig. 5. It is obvious from Figs. 4 and 5 that at the beginning the field corresponds to the OF LP_{01} eigenmode as we originally assumed. As the core of the IF shrinks, the field profile changes and the overlap integral decreases. The position of the splice is clearly visible. In the tapered MF the field is initially expanded and then compressed back and the overlap gradually increases.

3. Experiment

We performed an experiment in order to verify the design and theoretical results. We limited the

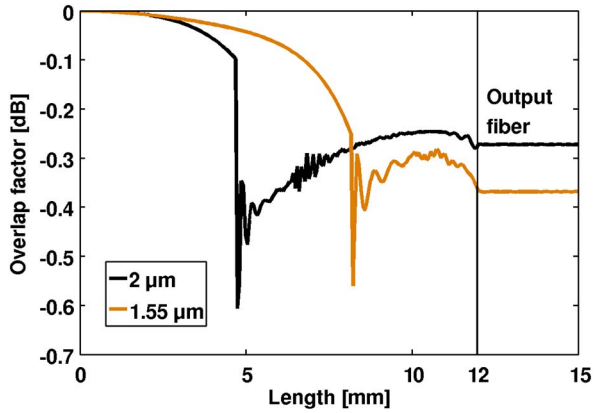

Fig. 4. Evolution of squared absolute value of the overlap integral between the output fiber LP_{01} eigenmode and the field in the taper along the structure.

verification only to the design for the wavelength of 1.55 μm due to ease of instrumentation.

A. Experimental Setup

We did not create the entire combiner in our experiments. We only verified whether tapering according to our design improves splicing loss between IF and MF, which is fundamental for our approach. At first, we spliced SMF28 and SCF-UN 20/125-12 fibers. We then tapered the spliced fibers according to our design using the VYTRAN GPX 3400 glass processing unit, see Fig. 6. The splice was placed in the narrowing part of the taper. The taper then continues and reaches the waist of a specific certain ratio. We created several tapers with different waist ratios. Beyond the waist the taper expands back to the original shape of the SCF-UN 20/125-12. Based on our simulations in Fig. 2, we assume that the field in the waist of the tapers corresponds to the OF field. Therefore, we did not investigate experimentally the connection between the taper and the OF. Instead, we assumed that expanding part of the taper is adiabatic and the transformation of the field to SCF-UN 20/125-12 is lossless. Thus, splicing loss between IF and MF does not depend on the waist diameter in this case.

We measured changes in transmission during the tapering process on the VYTRAN unit. Radiation of the wavelength of 1.55 μm was introduced into the SMF28 fiber. The end of SCF-UN 20/125-12 was connected to an InGaAs detector and its signal was observed using an oscilloscope set to slow time base.

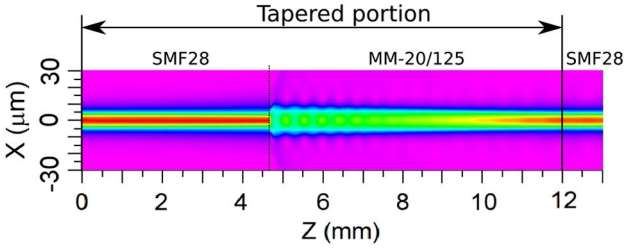

Fig. 5. Optical intensity evolution along the tapered section for the wavelength of 2 μm.

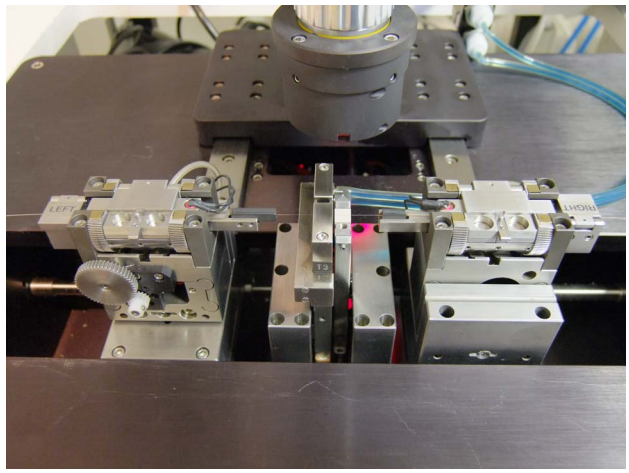

Fig. 6. Photo of the optical fiber tapering rig in the VYTRAN GPX 3400 device. The fiber is heated by an Ω-shaped graphite filament (under the shield in the middle) and pulled by the moveable fiber holders.

B. Experimental Results

The first example of the fabricated tapers (taper 1) had the waist diameter of 69 μm. This waist diameter corresponds to the taper ratio of 0.55. This is according to our simulations an optimal ratio for the splicing point between IF and MF, see Fig. 3.

The splice itself was positioned 3.5 mm before the waist, where the ratio of about 0.61 was achieved. The shape of the tapered splice is shown in Fig. 7. Figure 7(a) is only illustrative, namely the core dimensions are exaggerated and the experimental fiber taper is not strictly linear. Figure 7(b) shows that the taper slope is not continuous across the splice, but there is a step. This is probably because of the different material properties of both fibers. Nevertheless, this step did not cause any decrease in transmission, as is discussed later.

We recorded the transmitted power during the tapering procedure, see Fig. 8. The figure shows an increase in transmittance and thus a reduction

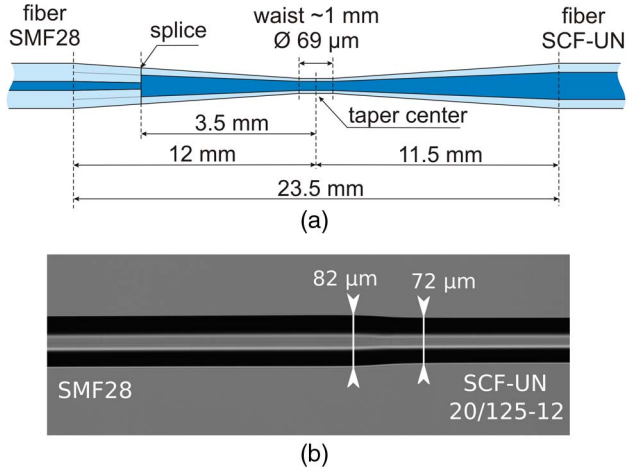

Fig. 7. (a) Dimensions of the taper 1, (b) detail of tapered splice inside the taper 1.

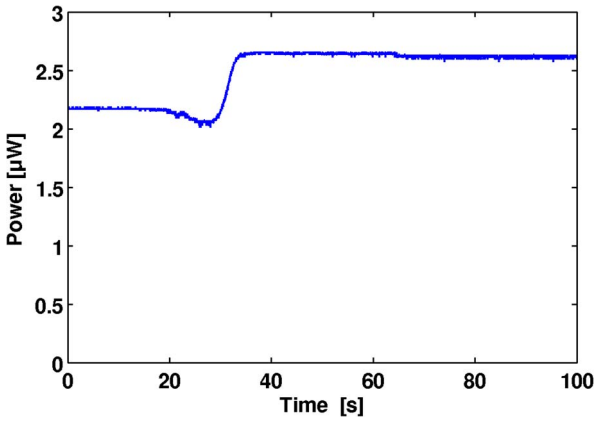

Fig. 8. Oscillogram of the tapering process of taper 1.

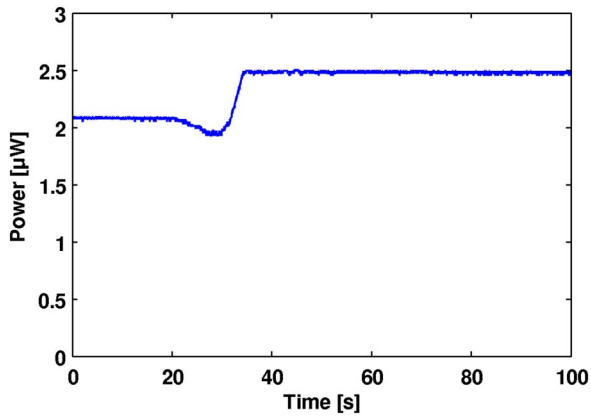

Fig. 10. Oscillogram of the tapering process of taper 2.

of splicing loss as the tapering head with the heat filament crossed the splice. Further phases of the tapering process had no significant impact on transmittance. This proves our assumptions concerning the independence on the waist diameter and the adiabatic field expansion back to SCF-UN 20/125-12.

The second taper example (taper 2) had the waist diameter of 50 μm. This corresponds to the ratio of 0.4, which is according to our simulations optimal for splicing to the OF, see Fig. 2. The position of the splice was 4.4 mm before the waist where the tapering ratio was approximately 0.54. This tapering ratio is very close to the optimal one, see Fig. 3. The taper shape and the tapering process oscillogram are shown in Figs. 9 and 10.

Improvement of splicing loss was slightly worse in taper 2 than in taper 1, as shown in Fig. 10. Taper 2 was thinner in diameter around the splice than taper 1. Although the splice diameter of this taper was closer to the optimal, it had higher loss than taper 1.

Figures 8 and 10 show only the improvement in splicing losses relative to the spliced fibers throughput. Finally, we also measured absolute losses of the tapered splices. A schematic of the measurement setup is shown in Fig. 11 [28]. At first the radiation

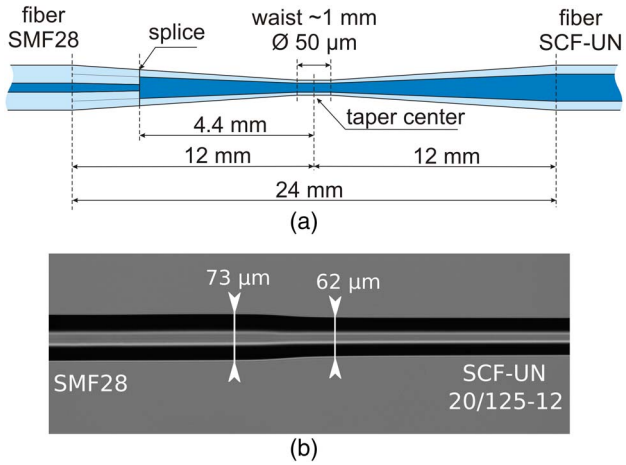

Fig. 9. (a) Dimensions of the taper 2, (b) detail of tapered splice inside the taper 2.

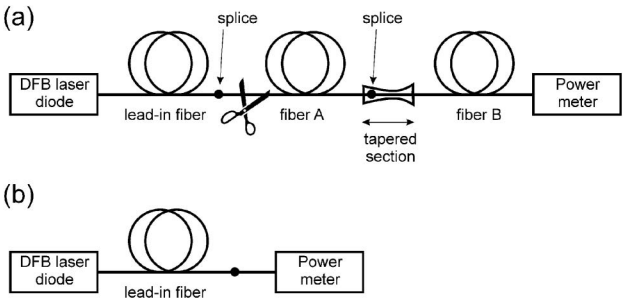

Fig. 11. Setup for the measurement of splice-losses: (a) Measurement of the optical power passing through the spliced dissimilar fiber A and B after tapering, (b) calibration of the input power.

was introduced from lead-in SMF28 fiber into SMF28 IF, and output power was measured at the end of intermediate SCF-UN 20/125-12 fiber. The input SMF28 fiber was then cleaved before taper and the input power was calibrated at this point. The difference of measured powers then gives loss of tapered splice. Lengths of all fibers were about 1 m. Measured losses are summarized in Table 1.

Table 1 shows better performance of the tapered splices than our theoretical simulations (see Fig. 3). Since the numerical simulations do not account for dopant diffusion it was expected that the experimental results should be better than the theoretical predictions based only on the mode-field overlap. While we assumed abrupt change in refractive index profiles between input and MFs in the numerical simulations, in real spliced and tapered structure the transition is more gradual due to dopant diffusion. Indeed, the advantageous impact of diffusion on reduction of splicing losses was also discussed in [20]. The difference between theoretical and experimental

Table 1. Losses of Created Taper Splices

	Measured Loss (dB)
Taper 1	0.02
Taper 2	0.17
Nontapered splice	0.98

results was probably also influenced by the fact that we used estimated equivalent step-index refractive index profiles of the input, intermediate, and OFs. Such approximated refractive index profiles may deviate from the real ones.

4. Conclusions

We presented to the best of our knowledge a novel type of a mode-field adapter for signal branch of pump and signal combiners. The principle and design procedure of the adapter was described using the examples of two particular adapters for the wavelengths of 2 and 1.55 μm and commercially available fibers. Numerical simulations showed insertion losses in the signal branch between the input single-mode fiber and the output DCF of 0.27 dB for the design wavelength of 2 μm and 0.37 dB for the design wavelength of 1.55 μm. The losses could be further improved using specially designed and optimized MFs.

We experimentally verified the fundamental principle of the adapter for the wavelength of 1.55 μm. We created two tapered splices between the IF and the MF. We observed improvement of splicing losses from 0.98 to 0.02 dB for the first taper and 0.17 dB for the second taper. Experimental results show even better performance than theoretical results as expected because of dopant diffusion during the splicing and tapering processes that was not accounted for in the numerical simulations. Especially, the important splice between significantly dissimilar input and MFs profits from dopant diffusion. The presented numerical and experimental results of the proposed mode-field adapter are promising for fabrication of high-power combiners with low signal losses.

This work was supported by the Czech Science Foundation, Project No. P205/11/1840, and by the Ministry of Industry and Trade of the Czech Republic, Project No. FR-TI4/734.

References

1. D. J. Richardson, J. Nilsson, and W. A. Clarkson, "High power fiber lasers: current status and future perspectives [Invited]," J. Opt. Soc. Am. B **27**, B63–B92 (2010).
2. E. Snitzer, H. Po, F. Hakimi, R. Tuminelli, and B. C. McCollumn, "Double-clad, offset core Nd fiber laser," in *Optical Fiber Sensors*, Vol. **2** of OSA Technical Digest Series (Optical Society of America, 1988), paper PD5.
3. F. Gonthier, L. Martineau, N. Azami, M. Faucher, F. Séguin, D. Stryckman, and A. Villeneuve, "High-power all-fiber components: the missing link for high power fiber lasers," Proc. SPIE **5335**, 266–276 (2004).
4. V. P. Gapontsev and L. E. Samartsev, "High-power fiber laser," in *Advanced Solid State Lasers*, G. Dube, ed., Vol. **6** of OSA Proceedings Series (Optical Society of America, 1990), paper LSR1.
5. V. P. Gapontsev and I. Samartsev, "Coupling arrangement between a multi-mode light source and an optical fiber through an intermediate optical fiber length," U.S. patent 5,999,673 (7 December 1999).
6. C. Jauregui, S. Bohme, G. Wenetiadis, J. Limpert, and A. Tünnermann, "Side-pump combiner for all-fiber monolithic fiber lasers and amplifiers," J. Opt. Soc. Am. B **27**, 1011–1015 (2010).
7. T. Weber, W. Lüthy, and H. Weber, "Side-pumped fiber laser," Appl. Phys. B **63**, 131–134 (1996).
8. Q. Xiao, P. Yan, H. Ren, X. Chen, and M. Gong, "Pump-signal combiner with large-core signal fiber feed-through for fiber lasers and amplifiers," Appl. Opt. **52**, 409–414 (2013).
9. P. Peterka, I. Kasik, V. Matejec, V. Kubecek, and P. Dvoracek, "Experimental demonstration of novel end-pumping method for double-clad fiber devices," Opt. Lett. **31**, 3240–3242 (2006).
10. P. Polynkin, V. Temyanko, M. Mansuripur, and N. Peyghambarian, "Efficient and scalable side pumping scheme for short high-power optical fiber lasers and amplifiers," IEEE Photon. Technol. Lett. **16**, 2024–2026 (2004).
11. A. B. Grudinin, J. Nilsson, P. W. Turner, C. C. Renaud, W. A. Clarkson, and D. N. Payne, "Single clad coiled optical fibre for high power lasers and amplifiers," in *Conference on Lasers and Electro-Optics*, OSA Technical Digest (Optical Society of America, 1999), paper CPD26.
12. M. N. Zervas and C. A. Codemard, "High power fiber lasers: a review," IEEE J. Sel. Top. Quantum Electron. **20**, 219–241 (2014).
13. D. J. DiGiovanni and A. J. Stentz, "Tapered fiber bundles for coupling light into and out of cladding-pumped fiber devices," U.S. patent 5,864,644 (26 January 1999).
14. F. Gonthier, F. Seigun, A. Villeneuve, M. Faucher, N. Azami, and M. Garneau, "Optical coupler comprising multimode fibers and method of making the same," U.S. patent 7,046,875 (16 May 2006).
15. V. P. Gapontsev, V. Fomin, and N. Platonov, "Fiber laser system," U.S. patent 7,848,368 (7 December 2010).
16. D. Neugroschl, J. Park, M. Wlodawski, J. Singer, and V. I. Kopp, "High-efficiency (6+1) × 1 combiner for high power fiber lasers and amplifiers," Proc. SPIE **8601**, 860139 (2013).
17. D. Noordegraaf, M. D. Maack, P. M. W. Skovgaard, S. Agger, T. T. Alkeskjold, and J. Lægsgaard, "7 + 1 to 1 pump/signal combiner for air-clad fiber with 15 μm MFD PM single-mode signal feed-through," Proc. SPIE **7580**, 75801A (2010).
18. B. G. Ward, D. L. Sipes, Jr., and J. D. Tafoya, "A monolithic pump signal multiplexer for air-clad photonic crystal fiber amplifiers," Proc. SPIE **7580**, 75801C (2010).
19. L. Kong, J. Leng, J. Cao, S. Guo, and H. Jiang, "The comparison between MFD and MOI on the simulation of combiner insertion loss," Proc. SPIE **8904**, 890416 (2013).
20. A. Oehler, T. Hauff, W. Heinlein, W. Stieb, and J. Schulte, "New field-matching technique for low-loss splices between conventional and dispersion-flattened single-mode fibres," in *Proceedings of the 14th European Conference on Optical Communication ECOC 88* (IEEE 1988), pp. 603–606.
21. N. Healy, E. McDaid, D. F. Murphy, C. D. Hussey, and T. A. Birks, "Low-loss single mode fibre 1 × 2 Y-junction," Electron. Lett. **42**, 740–742 (2006).
22. CorActive High Tech Inc., "Passive fibers brochure," www.coractive.com/pdf/brochures/PassiveFibers_BR0004r06.pdf.
23. D. Schulz, C. Glingener, M. Bludszuweit, and E. Voge, "Mixed finite element beam propagation method," J. Lightwave Technol. **16**, 1336–1342 (1998).
24. C. Geuzaine and J. F. Remacle, "Gmsh: a three-dimensional finite element mesh generator with built-in pre- and post-processing facilities," Int. J. Numer. Methods Eng. **79**, 1309–1331 (2009).
25. T. A. Birks and Y. W. Li, "The shape of fiber tapers," J. Lightwave Technol. **10**, 432–438 (1992).
26. A. W. Snyder and J. D. Love, *Optical Waveguide Theory* (Chapman and Hall, 1983), pp. 420–441.
27. A. D. Yablon, *Optical Fiber Fusion Splicing* (Springer, 2005), pp. 91–135.
28. D. Derickson, *Fiber Optic Test and Measurement* (Prentice-Hall, 1998), Chap. 9.